

Multi-stage Co-planning Model for Power Distribution System and Hydrogen Energy System Under Uncertainties

Qirun Sun, Zhi Wu, Wei Gu, Pengxiang Liu, Jingxuan Wang, Yuping Lu, Shu Zheng, and Jingtao Zhao

Abstract—The increased deployment of electricity-based hydrogen production strengthens the coupling of power distribution system (PDS) and hydrogen energy system (HES). Considering that power to hydrogen (PtH) has great potential to facilitate the usage of renewable energy sources (RESs), the coordination of PDS and HES is important for planning purposes under high RES penetration. To this end, this paper proposes a multi-stage co-planning model for the PDS and HES. For the PDS, investment decisions on network assets and RES are optimized to supply the growing electric load and PtHs. For the HES, capacities of PtHs and hydrogen storages (HSs) are optimally determined to satisfy hydrogen load considering the hydrogen production, tube trailer transportation, and storage constraints. The overall planning problem is formulated as a multi-stage stochastic optimization model, in which the investment decisions are sequentially made as the uncertainties of electric and hydrogen load growth states are revealed gradually over periods. Case studies validate that the proposed co-planning model can reduce the total planning cost, promote RES consumption, and obtain more flexible decisions under long-term load growth uncertainties.

Index Terms—Power distribution system, vehicle-based hydrogen energy system, co-planning model, multi-stage stochastic programming, uncertainty.

NOMENCLATURE

A. Indices and Sets

τ Index of power distribution system (PDS) scheduling time period

τ' Index of hydrogen energy system (HES) scheduling time period

Ω_a^L Set of head and tail nodes in power lines a

Ω_c Set of uncertain scenarios

$\Omega_i^{L+}/\Omega_i^{L-}$ Set of power lines with node i as head/tail

Ω_i Set of planning stages

$\Omega_{\text{HN}}/\Omega_{\text{HL}}/\Omega_{\text{HT}}^g$ Set of hydrogen nodes/hydrogen loads/HTs

$\Omega_{\text{SS}}/\Omega_{\text{L}}/\Omega_{\text{PV}}/$
 $\Omega_{\text{WT}}/\Omega_{\text{PH}}/\Omega_{\text{HS}}/$
 Ω_{HT} Set of substations/power lines/photovoltaics (PVs)/wind turbines (WTs)/power to hydrogens(PtHs)/hydrogen storages (HSs)/HTs

Ω_{PH}^i Set of hydrogen nodes corresponding to PtH node i

$\Omega_{\text{PN}}/\Omega_{\text{PL}}/\Omega_{\text{Tra}}$ Set of power nodes/power loads/transportation paths

$a/(i, j)$ Index of power lines

d Index of hydrogen tube trailer (HT)

g Index of HGS

i/j Index of power nodes including generation station (HGS) and hydrogen refueling station (HRS)

$K_{\text{TR}}/K_{\text{L}}$ Set of candidate transformers/power line types

m/n Index of hydrogen nodes including HGS and HRS

s Index of operating scenario

t/v Index of planning stages

B. Parameters

ψ Annual interest rate

γ_t Initial year

$\rho_{\text{SS}}/\rho_{\text{TR}}/\rho_{\text{L}}/\rho_{\text{PV}}/$
 $\rho_{\text{WT}}/\rho_{\text{PH}}/\rho_{\text{HS}}$ Capital recovery rate of substation/transformer/power line/PV/WT/PtH/HS

$\Delta_t/\Delta_{\tau'}$ Duration of time period

λ^{Loss} Network loss cost coefficient of PDS

$\lambda_{\tau'}$ Travel cost of HTs per km

Manuscript received: June 6, 2022; revised: September 6, 2022; accepted: September 27, 2022. Date of CrossCheck: September 27, 2022. Date of online publication: October 26, 2022.

This work was supported in part by the Postgraduate Research & Practice Innovation Program of Jiangsu Province (No. KYCX22_0258) and in part by the National Natural Science Foundation of China (No. 52177077).

This article is distributed under the terms of the Creative Commons Attribution 4.0 International License (<http://creativecommons.org/licenses/by/4.0/>).

Q. Sun, Z. Wu (corresponding author), W. Gu, P. Liu, J. Wang, and Y. Lu are with School of Electrical Engineering, Southeast University, Nanjing 210096, China (e-mail: 230218326@seu.edu.cn; zwu@seu.edu.cn; wgu@seu.edu.cn; px-liu_phd@seu.edu.cn; 220202922@seu.edu.cn; luyuping@seu.edu.cn).

S. Zheng and J. Zhao are with NARI Technology Development Co. Ltd, Nanjing, China (e-mail: zhengshu@sgepri.sgcc.com.cn; zhaojingtao@sgepri.sgcc.com.cn).

DOI: 10.35833/MPCE.2022.000337



λ_d^{Dis}	Fixed dispatch cost for HT d	$\bar{S}_k^L/\bar{S}_k^{\text{TR}}$	Capacity of power line/transformer in type k
μ_{HS}	Installed import (export) to capacity ratios of HS	\underline{U}/\bar{U}	Lower/upper bound for nodal voltage
μ_{ex}	The maximum hydrogen export ratio	$\bar{X}_{ii}^{\text{PV}}/\bar{X}_{ii}^{\text{WT}}/\bar{X}_{ii}^{\text{PtH}}/$	Upper bound for installed PV/WT/PtH/HS
$\varphi_{\text{SS}}/\varphi_{\text{PL}}/\varphi_{\text{PV}}/$ φ_{WT}	Power factor of substation/power load/PV/WT	\bar{X}_{ii}^{HS}	
$\zeta_{st}^{\text{PV}}/\zeta_{st}^{\text{WT}}/\zeta_{st}^{\text{PL}}/$ $\zeta_{st}^{\text{HL}}/$	Level of PV/WT/power load/hydrogen load	<i>C. Variables</i>	
μ	The maximum penetration rate of RES	$\alpha_{idst}^{m,n}$	Binary state variable of HT d between m and n
$\delta/\bar{\delta}$	Lower/upper capacity level of HSs	β_{idst}^m	Auxiliary variable of HT d at hydrogen node m
$\varsigma_{\text{CP}}/\varsigma_{\text{CH}}$	The maximum curtailed rate of power/hydrogen load	$c_i^I/c_i^M/c_i^O/c_i^U$	Investment/maintenance/operation/unserved energy cost
$\eta_{\text{PtH}}/\eta_{\text{Com}}$	PtH efficiency/power consumption rate of compressor	$E_{gst}^{\text{HGS}}/E_{mst}^{\text{HRS}}$	Hydrogen level of HS
$ \Omega_{\text{HN}} / \Omega_{\text{PL}} /$ $ \Omega_i $	Number of hydrogen node/power load node/planning stage	f_{ia}^L	Fictitious power flow through power line a
$C_i^{\text{I,SS}}$	Investment cost coefficient of substation	$f_{ii}^{\text{SS}}/f_{ii}^{\text{PL}}$	Fictitious power of substation/power load
$C_k^{\text{I,TR}}/C_k^{\text{I,LL}}$	Investment cost coefficient of transformer/power line in type k	$h_{gst}^{\text{ch}}/h_{gst}^{\text{dis}}$	Charged/discharged hydrogen of HS
$C_t^{\text{I,PV}}/C_t^{\text{I,WT}}/$ $C_t^{\text{I,PtH}}/C_t^{\text{I,HS}}$	Investment cost coefficient of PV/WT/PtH/HS	h_{gst}^{ex}	Hydrogen exported from PtH to HT
$C_i^{\text{M,SS}}$	Maintenance cost coefficient of substations at power node i	$h_{mst}^{\text{im},d}$	Hydrogen imported from HT d to HRS m
$C_k^{\text{M,TR}}/C_k^{\text{M,LL}}$	Maintenance cost coefficient of transformer/power line in type k	$h_{gst}^{\text{toHT},d}$	Hydrogen exported to HT d
$C_t^{\text{M,PV}}/C_t^{\text{M,WT}}/$ $C_t^{\text{M,PtH}}/C_t^{\text{M,HS}}$	Maintenance cost coefficient of PV/WT/PtH/HS	h_{gst}^{PtH}	Hydrogen produced by PtH
$C_i^{\text{O,SS}}$	Electricity purchase cost from substation	I_{ast}^L	Square of current through power line a
$C^{\text{O,PV}}/C^{\text{O,WT}}$	Production cost of PV/WT	$p_{ist}^{\text{SS}}/p_{ist}^{\text{PV}}/p_{ist}^{\text{WT}}$	Active power injected by substation/PV/WT
$C_{\tau}^{\text{O,PtH}}$	Electricity purchase cost of PtHs	$p_{ist}^{\text{PtH}}/p_{ist}^{\text{Com}}$	Active power consumed by PtH/compressor
$C^{\text{U,D}}/C^{\text{U,H}}$	Unserved cost of power/hydrogen load	$p_{ist}^{\text{CD}}/h_{mst}^{\text{CD}}$	Unserved power/hydrogen load
$C^{\text{U,PV}}/C^{\text{U,WT}}$	Curtailed cost of PV/WT	$p_{ast}^L/q_{ast}^L/s_{ast}^L$	Active/reactive/apparent power flow through power line a
D_s	Number of day	$p_{ist}^{\text{CPV}}/p_{ist}^{\text{CWT}}$	Curtailed active power of PV/WT
$h_{mst}^{\text{D}}/H_{mt}^{\text{D}}$	Hourly/base hydrogen load of m	$q_{ist}^{\text{SS}}/q_{ist}^{\text{PV}}/q_{ist}^{\text{WT}}$	Reactive power injected by substation/PV/WT
$\bar{H}_{\text{in}}^{\text{HT}}/\bar{H}_{\text{out}}^{\text{HT}}$	The maximum loading/unloading hydrogen of HT d	U_{ist}	Square of voltage
\bar{I}_k^L	Upper bound for current through the power line	$x_{it}^{\text{SS}}/x_{ikt}^{\text{TR}}/x_{akt}^L$	Binary investment variables for substation/transformer/power line
l_a	Length of power line	$x_{it}^{\text{PV/WT}}$	Investment variable for PV/WT
$l_{m,n}$	Distance between m and n	$x_{gt}^{\text{PtH}}/x_{mt}^{\text{HS}}$	Investment variable for PtH/HS
M	A large positive number	$y_{at}^{\text{L+}}/y_{at}^{\text{L-}}$	Binary forward/backward utilization variable for power line a
N_{τ}	Number of time periods within a typical day		
$p_{ist}^{\text{D}}/P_{it}^{\text{D}}$	Hourly/base power load of i		
$P_{l,c}$	Probability of scenario c		
R_a/X_a	Resistance/reactance of power line a		

I. INTRODUCTION

WITH the global concern for greenhouse gas emissions, clean and low-carbon renewable energy sources (RESs) are gradually replacing traditional fossil energy [1]. In the future RES-dominated power distribution system (PDS), how to effectively consume fluctuating RES while eliminating the adverse effects needs to be properly addressed [2]. Recently, with the development of power-to-hydrogen (PtH) technologies, electric hydrogen production is recognized as a promising way to accommodate the intermittent and volatile RES in PDS [3]. As an interface between PDS and hydrogen energy system (HES), the growing PtHs

significantly enhance the coupling relationships of PDS and HES, and establish the integrated power distribution and hydrogen system (IPDHS) [4].

Considering that PDS and HES have significant synergistic effects, several research works have been conducted on the coordinated operation of IPDHS. In [5], a mixed-integer linear programming (MILP) based optimal operation model is developed for a wind-electrolytic IPDHS, which can relieve the uncertainties of wind power outputs and obtain economic profits. In [6], an optimal IPDHS scheduling model that considers the variable RES, hydrogen refueling stations (HRSs), and hydrogen tube trailers (HTs) is proposed, and numerical studies demonstrate its effectiveness in increasing the system operational flexibility under high RES penetration. Reference [7] establishes a coordinated power system and HES operation model to resist the output variabilities of RES, which can effectively lower the dispatch costs of the overall system. In [8], an optimal IPDHS operation model is proposed considering the PDS operation, HT-based hydrogen transportation and demand response of hydrogen loads, which can achieve efficient resource allocation and economic benefits. In [9], the spatial-temporal distribution of hydrogen vehicles is incorporated into the IPDHS scheduling framework, and numerical results prove that the coordination of two systems can obtain significant economic and environmental benefits.

The above studies prove the significant benefits through the coordinated operation of PDS and HES. However, they mainly focus on the operation level. In view of the above merits, joint optimal planning of IPDHS is urgently needed to benefit both PDS and HES. In general, the planning problems of PDS and HES have been widely studied in the existing literature in a separate manner. For the former, the planning strategies for PDS with high RES penetration have been well investigated such as [10]-[15]. Generally, the PDS planning is to upgrade the system assets to satisfy the growing demand while responding to the technical and security constraints, which is a complex mixed-integer non-linear problem. In terms of modeling formulations, various approaches have been developed. In [10], a joint PDS and renewable energy expansion planning model that considers demand response and energy storage is developed, and the overall problem is linearized and formulated as a scenario-based stochastic MILP model. Reference [11] proposes an MILP-based AC/DC hybrid PDS planning model to resist long-term load growth uncertainties, in which the power line thermal quadratic constraints are linearized by several square constraints. In [12], a bi-level multi-objective RES and energy storage co-planning model is developed considering both RES and power load uncertainties. In [13], a multi-stage PDS expansion planning model is developed to integrate multiple RES, and the overall problem is modeled and solved by an approximate dynamic programming method. In [14], a security-constrained AC/DC hybrid PDS expansion planning model is established to accommodate the high penetration of RES in weak grids, and the overall problem is formulated as a mixed-integer second-order cone programming (MISOCP) model. Reviewed from the aspect of solution

techniques, the commonly-used methods in existing literature can be divided into three groups: mathematical optimization methods [10], [11], [14], heuristic methods [12], and hybrid algorithms [15]. As for mathematical optimization methods, it can formulate PDS planning problems into tractable models and solve them with efficient off-the-shelf software. The heuristic methods and hybrid algorithms can be utilized to solve large-scale PDS planning models with high computation burdens, but the global optimalities of the solutions cannot be guaranteed. In the existing studies, the PTHs have not been considered in PDS planning problems. In essence, PTHs can be viewed as a new type of power load in PDS [16], which can promote RES utilization and provide additional flexibility in operations. Therefore, the proper deployment of PTHs has great potential to reduce the expansion burden of PDS with high RES penetration.

For the HES planning problems, researchers have developed meaningful works. Generally, the HES consists of hydrogen production, transportation, and storage sectors. Considering the scale merit of PTHs, centralized hydrogen generation is widely designed to lower hydrogen production costs, and hydrogen storage (HS) is utilized to increase operational flexibility. In [17], a robust electricity-hydrogen integrated energy system planning model is proposed, which considers on-site hydrogen production and storage technologies to promote RES consumption. In [18], the centralized hydrogen production is discussed in a PDS, and a local energy market is planned for power and hydrogen loads. However, the above studies only consider the hydrogen production and storage sections, while the hydrogen transportation is neglected. Different from the electricity in power systems, hydrogen is delivered via pipes or HTs with pressured tanks, and the hydrogen transportation cost accounts for a large proportion of the total hydrogen cost. In view of this, several studies such as [19]-[22] have considered the hydrogen transportation section in HES planning problems. In [19], a hydrogen supply chain planning model is developed, which considers the hydrogen production, storage, and transmission facilities to meet hydrogen loads. Reference [20] establishes an HES planning model considering PTHs, pipeline delivery and HRSs, which can obtain a coordinated planning scheme with cheaper hydrogen costs and higher RES consumption. In [21], a joint power transmission system and HES planning model is developed to achieve resource complementation, in which the hydrogen is flexibly delivered by pipelines and HTs. Reference [22] develops a multi-regional energy station planning method that considers the interconnection of power transmission system and HES, in which the hydrogen is transported across multiple regions. However, [19] does not consider the operational constraints of the power system, which may restrict the operation of PTHs. References [20]-[22] focus on the power transmission level rather than the distribution level. The aforementioned research works provide significant insights into power-hydrogen interactions in planning problems. However, to the best of our knowledge, the PDS expansion as well as the HES production, transportation and storage planning have not been jointly considered in the existing studies.

As discussed above, little attention has been paid to the joint planning of PDS under high RES penetration and HES with consideration of the production, transportation, and storage sections. There are three main gaps in the existing literature: the coordinated planning of PDS and HES has not been fully considered, and how to take advantage of the synergy between them to reduce the planning cost and facilitate RES consumption has not been explored; the role of HES operation flexibility can be further exploited in the co-planning framework, in which hydrogen production, transportation, and storage can be coordinated with PDS to increase the system operational flexibility; and the IPDHS co-planning is a multi-period problem with long-term planning horizon, and the load growth uncertainties of power and hydrogen deserve to be considered.

This paper proposes a multi-stage stochastic IPDHS co-planning model under long-term load growth uncertainties, and the main contributions are summarized below.

1) A novel multi-stage stochastic IPDHS co-planning model is proposed to optimize the PDS expansion and HES configuration, in which various energy devices can be coordinately deployed to meet the power/hydrogen loads economically.

2) HES including PtH, HS, and HT transportations is coordinated with variable photovoltaics (PVs) and wind turbines (WTs) in PDS, and the flexible operation of HES can effectively promote RES utilization, relieve PDS expansion burden, and reduce the planning cost of the overall system.

3) A multi-stage stochastic model with non-anticipativity constraints is set up for the IPDHS co-planning problem to address long-term load uncertainties, in which the investment decisions are sequentially made as the load growths of power and hydrogen are revealed gradually over periods.

The rest of this paper is organized as follows. Section II illustrates the proposed IPDHS co-planning framework. Section III presents the mathematical formulation of the co-planning model, followed by the solution algorithm in Section IV. Numerical studies are carried on Section V, and Section VI draws the conclusions.

II. PROPOSED IPDHS CO-PLANNING FRAMEWORK

The proposed IPDHS co-planning framework is shown in Fig. 1. Considering that hydrogen pipeline is expensive and the construction of new pipelines in urban areas of PDS is difficult [7], this paper considers a vehicle-based HES. The HES mainly composes hydrogen generation stations (HGSs) for hydrogen production, HTs for hydrogen transportation, and hydrogen loads. The PDS and HES are coupled by the PtHs. Within HGS, PtHs can convert surplus electricity into hydrogen, which can be viewed as flexible loads in the PDS.

In the proposed co-planning framework, substations, power lines, photovoltaics (PVs), and wind turbines (WTs) in the PDS as well as PtHs and HSs in the HES are invested to supply the growing power and hydrogen loads over periods. For the HES, the flexible operation of PtHs with HSs can promote the utilization of variable RES and produce hydrogen with cheaper electricity costs. Besides, by optimizing the locations and capacities of PtHs, the expansion burden of PDS can be potentially relieved.

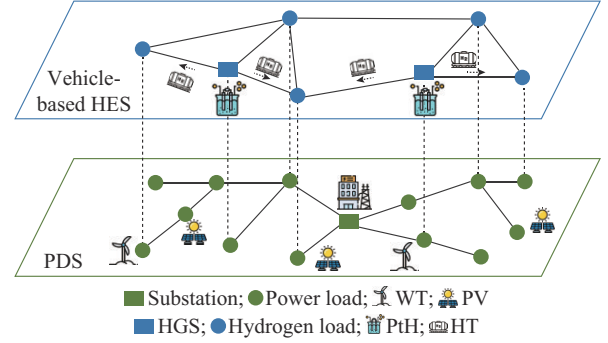


Fig. 1. Proposed IPDHS co-planning framework.

III. MATHEMATICAL FORMULATION

The proposed co-planning framework is based on the following assumptions and premises: ① the distribution system operator (DSO) serves as the centralized planner and the information of the HES is available to the DSO; ② the planning horizon is divided into $|\Omega_t|$ stages, and a fixed annual interest rate is considered; ③ typical scenarios in summer, winter and transition seasons are utilized to model the stochastic characteristics of PVs, WT, and power/hydrogen loads; and ④ the transportation process of HTs is modeled as a vehicle routing problem [7], [8].

A. Objective Function and Cost-related Terms

The objective of the proposed co-planning framework is to minimize the present value of total costs over the planning horizon, as shown in (1).

$$\min f = \sum_{t \in \Omega_t} \frac{1}{(1+\psi)^{y_t}} (c_t^I + c_t^M + c_t^O + c_t^U) \quad (1)$$

$$\begin{aligned} c_t^I = & \sum_{i \in \Omega_{SS}} x_{it}^{SS} C_i^{L,SS} \rho_{SS} + \sum_{i \in \Omega_{SS}} \sum_{k \in K_{TR}} x_{ikt}^{TR} C_k^{I,TR} \rho_{TR} + \\ & \sum_{a \in \Omega_L} \sum_{k \in K_L} x_{akt}^{L} C_k^{I,L} l_a \rho_L + \sum_{i \in \Omega_{PV}} (x_{it}^{PV} - x_{i,t-1}^{PV}) C_t^{I,PV} \rho_{PV} + \\ & \sum_{i \in \Omega_{WT}} (x_{it}^{WT} - x_{i,t-1}^{WT}) C_t^{I,WT} \rho_{WT} + \sum_{g \in \Omega_{PH}} (x_{gt}^{PH} - x_{g,t-1}^{PH}) \cdot \\ & C_t^{I,PH} \rho_{PH} + \sum_{m \in \Omega_{HN}} (x_{mt}^{HS} - x_{m,t-1}^{HS}) C_t^{I,HS} \rho_{HS} \end{aligned} \quad (2)$$

$$\begin{aligned} c_t^M = & \sum_{i \in \Omega_{SS}} x_{it}^{SS} C_i^{M,SS} + \sum_{i \in \Omega_{SS}} \sum_{k \in K_{TR}} x_{ikt}^{TR} C_k^{M,TR} + \\ & \sum_{a \in \Omega_L} (y_{at}^{L+} + y_{at}^{L-}) l_a C_k^{M,L} + \sum_{i \in \Omega_{PV}} x_{it}^{PV} C_t^{M,PV} + \\ & \sum_{i \in \Omega_{WT}} x_{it}^{WT} C_t^{M,WT} + \sum_{g \in \Omega_{PH}} x_{gt}^{PH} C_t^{M,PtH} + \sum_{m \in \Omega_{HN}} x_{mt}^{HS} C_t^{M,HS} \end{aligned} \quad (3)$$

$$\begin{aligned} c_t^O = & \sum_s D_s \left(\sum_{\tau} A_{\tau} \left[\sum_{i \in \Omega_{SS}} C_{\tau}^{O,SS} p_{isst}^{SS} + \sum_{a \in \Omega_L} \lambda^{Loss} I_{dst}^{L} R_a + \right. \right. \\ & \sum_{i \in \Omega_{PV}} C_{\tau}^{O,PV} p_{isst}^{PV} + \sum_{i \in \Omega_{WT}} C_{\tau}^{O,WT} p_{isst}^{WT} + C_{\tau}^{O,PtH} \cdot \\ & \left. \left. (p_{isst}^{PtH} + p_{isst}^{Com}) \right] + \sum_{\tau'} \sum_{d \in \Omega_{HT}} \left[\sum_{m \in \Omega_{Tra}} \lambda_{\tau'}^{Tra} \alpha_{dst}^{m,n} l_{mn} + \right. \right. \\ & \left. \left. \sum_{g \in \Omega_{PH}} \sum_{m \in \Omega_{HL}} \lambda_d^{Dis} \alpha_{dst}^{g,m} \right] \right) \end{aligned} \quad (4)$$

$$c_t^U = \sum_s D_s \sum_\tau A_\tau \left(\sum_{i \in \Omega_{PL}} C^{U,D} p_{ist}^{CD} + \sum_{i \in \Omega_{PV}} C^{U,PV} p_{ist}^{CPV} + \sum_{i \in \Omega_{WT}} C^{U,WT} p_{ist}^{CWT} + \sum_{m \in \Omega_{HL}} C^{U,H} h_{mst}^{CD} \right) \quad (5)$$

$$\rho_\sigma = \psi(1+\psi)^{Y_\sigma} / [(1+\psi)^{Y_\sigma} - 1] \quad \sigma \in \{SS, TR, L, PV, WT, PtH, HS\} \quad (6)$$

Equation (2) represents the investment cost, which comprises seven terms related to the installation of new substations, transformers, power lines, PVs, WTs, PtHs, and HSs, respectively. In (3), the maintenance costs for all the devices are formulated. In (4), the operation costs in PDS comprise the electricity purchase cost, the PDS network loss cost, and the RES operation cost, while the operation costs in HES contain the PtH operation cost and hydrogen transportation cost (including HT travel cost and fixed dispatch cost). Equation (5) represents the penalty costs for power/hydrogen load shedding and RES curtailment. The capital recovery rate for each device is calculated in (6), where Y_σ is the lifetime of each device in a year.

B. Constraints

1) Investment constraints: constraints of investment decisions are formulated in (7)-(13). Constraints (7)-(9) present the binary nature of investment decisions for substations, transformers, and power lines, respectively. Besides, only one investment of the candidate alternatives is allowed for each device throughout the planning horizon. Constraint (10) ensures that the investment for PVs, WTs, PtHs, and HSs will exist if it has been installed previously, while constraint (11) imposes the upper bounds on them at each planning stage. Constraints (12) and (13) restrict that the transformers and power lines cannot be installed on the attached substations that have not been built.

$$\sum_{i \in \Omega_i} x_{it}^{SS} \leq 1 \quad \forall i \in \Omega_{SS}, x_{it}^{SS} \in \{0, 1\} \quad (7)$$

$$\sum_{i \in \Omega_i} \sum_{k \in K_{TR}} x_{ikt}^{TR} \leq 1 \quad x_{ikt}^{TR} \in \{0, 1\}, \forall i \in \Omega_{SS} \quad (8)$$

$$\sum_{i \in \Omega_i} \sum_{k \in K_L} x_{akt}^L \leq 1 \quad x_{akt}^L \in \{0, 1\}, \forall a \in \Omega_L \quad (9)$$

$$x_{i,t-1}^\sigma \leq x_{it}^\sigma \quad \forall i \in \Omega_\sigma, t, \sigma \in \{PV, WT, PtH, HS\} \quad (10)$$

$$x_{it}^\sigma \leq \bar{X}_{it}^\sigma \quad \forall i \in \Omega_\sigma, t, \sigma \in \{PV, WT, PtH, HS\} \quad (11)$$

$$\sum_{v \leq t} \sum_{k \in K_{TR}} x_{ikv}^{TR} \leq \sum_{v \leq t} x_{iv}^{SS} \quad \forall i \in \Omega_{SS}, t \quad (12)$$

$$\sum_{v \leq t} \sum_{k \in K_L} x_{akv}^L \leq \sum_{v \leq t} x_{iv}^{SS} \quad \forall i \in \Omega_{SS}, a \in \Omega_i^L \cup \Omega_i^{L-}, t \quad (13)$$

2) PDS constraints: PDS operation constraints are formulated based on the DistFlow model [23]. Active and reactive power balance equations are stated as in (14) and (15), respectively. Constraint (16) relates nodal voltage drop to the active and reactive power flow across the power lines, and the Big- M method [13] is utilized to invalidate the constraints for non-operation lines. Constraints (17) and (18) relate active, reactive and apparent power flows on the lines,

and restrict their relations to the nodal voltage and the current flow. It should be noted that (17) and (18) are relaxed by replacing the equal sign with the smaller-than-or-equal sign. After relaxation, constraints (17) and (18) are convex second-order cone constraints [24]. The second-order cone relaxation is exact since the planning model meets the sufficient conditions presented in [25]. Capacity limits for power lines are defined in (19), and active power limits for substations are restrained in (20). Constraints (21) and (22) specify the limits for nodal voltage and the current through power lines, respectively. Boundaries for RES active outputs and curtailed power are constrained in (23) and (24). Reactive power of substations, PVs, and WTs is restricted in (25). Active power loads and the maximum curtailed loads are defined in (26). Constraint (27) specifies the active power limits of PtHs. Constraint (28) restricts the RES penetration level to maintain the operational safety of the PDS.

$$\sum_{a \in \Omega_i^+} (p_{atst}^L - I_{atst}^L R_a) - \sum_{a \in \Omega_i^+} p_{atst}^L + p_{istt}^{SS} + p_{istt}^{PV} + p_{istt}^{WT} - p_{istt}^{PtH} - p_{istt}^{Com} = p_{istt}^D - p_{istt}^{CD} \quad \forall i \in \Omega_{PN}, t, s, \tau \quad (14)$$

$$\sum_{a \in \Omega_i^+} (q_{atst}^L - I_{atst}^L X_a) - \sum_{a \in \Omega_i^+} q_{atst}^L + q_{istt}^{SS} + q_{istt}^{PV} + q_{istt}^{WT} = (p_{istt}^D - p_{istt}^{CD}) \tan \varphi_{PL} \quad \forall i \in \Omega_{PN}, t, s, \tau \quad (15)$$

$$-M(1 - y_{at}^{L+} - y_{at}^{L-}) \leq U_{istt} - U_{jstt} - 2(p_{atst}^L R_a + Q_{atst}^L X_a) + I_{atst}^L (R_a^2 + X_a^2) \leq M(1 - y_{at}^{L+} - y_{at}^{L-}) \quad \forall a \in \Omega_L, (i, j) \in \Omega_a^L, t, s, \tau \quad (16)$$

$$(p_{atst}^L)^2 + (q_{atst}^L)^2 \leq (s_{atst}^L)^2 \quad \forall a \in \Omega_L, t, s, \tau \quad (17)$$

$$(s_{atst}^L)^2 \leq I_{atst}^L U_{istt} \quad \forall a \in \Omega_i^L, t, s, \tau \quad (18)$$

$$0 \leq s_{atst}^L \leq \sum_{v \leq t} \sum_{k \in K_L} x_{akv}^L \bar{S}_k^L \quad \forall a \in \Omega_L, t, s, \tau \quad (19)$$

$$0 \leq p_{istt}^{SS} \leq \sum_{v \leq t} \sum_{k \in K_{TR}} x_{ikv}^{TR} \bar{S}_k^{TR} \quad \forall i \in \Omega_{SS}, t, s, \tau \quad (20)$$

$$\underline{U}^2 \leq U_{istt} \leq \bar{U}^2 \quad \forall i \in \Omega_{PN}, t, s, \tau \quad (21)$$

$$0 \leq I_{atst}^L \leq (\bar{I}_k^L)^2 x_{akt}^L \quad \forall a \in \Omega_L, t, s, \tau \quad (22)$$

$$\begin{cases} p_{istt}^{PV} \geq 0 \\ p_{istt}^{CPV} \leq \zeta_{st}^{PV} x_{it}^{PV} \\ p_{istt}^{PV} + p_{istt}^{CPV} = \zeta_{st}^{PV} x_{it}^{PV} \\ 0 \leq p_{istt}^{WT} \end{cases} \quad \forall i \in \Omega_{PV}, t, s, \tau \quad (23)$$

$$\begin{cases} p_{istt}^{CWT} \leq \zeta_{st}^{WT} x_{it}^{WT} \\ p_{istt}^{WT} + p_{istt}^{CWT} = \zeta_{st}^{WT} x_{it}^{WT} \end{cases} \quad \forall i \in \Omega_{WT}, t, s, \tau \quad (24)$$

$$-p_{istt}^\sigma \tan \varphi_\sigma \leq q_{istt}^\sigma \leq p_{istt}^\sigma \tan \varphi_\sigma \quad \forall i \in \Omega_\sigma, \sigma \in \{SS, PV, WT\}, t, s, \tau \quad (25)$$

$$\begin{cases} p_{istt}^D = \zeta_{st}^{PL} P_{it}^D \\ 0 \leq p_{istt}^{CD} \leq \zeta_{CP} p_{istt}^D \end{cases} \quad \forall i \in \Omega_{PL}, t, s, \tau \quad (26)$$

$$0 \leq p_{istt}^{PtH} \leq x_{it}^{PtH} \quad \forall i \in \Omega_{PtH}, t, s, \tau \quad (27)$$

$$\sum_{i \in \Omega_{PV}} p_{istt}^{PV} + \sum_{i \in \Omega_{WT}} p_{istt}^{WT} \leq \mu \sum_{i \in \Omega_{PL}} p_{istt}^D \quad \forall t, s, \tau \quad (28)$$

The network radiality of PDS is constrained in (29)-(36). Constraint (29) restricts that the power lines cannot operate

in two directions simultaneously, while constraint (30) ensures that the uninstalled power lines cannot operate. Constraints (31) and (32) model the PDS operation topology as a tree structure. To be specific, the substation and load nodes are modeled as parent and child nodes, respectively. Furthermore, to avoid the isolated areas formed by the RES, fictitious power flow constraints (33)-(36) are introduced, which ensures that each load node has one substation as the parent node [14]. Equation (33) denotes the fictitious power nodal balance equation, and the boundaries for fictitious power variables on power lines, power loads, and substations are defined in (34)-(36).

$$y_{at}^{L+} + y_{at}^{L-} \leq 1 \quad \forall a \in \Omega_L, t \quad (29)$$

$$y_{at}^{L+} + y_{at}^{L-} \leq \sum_{v \leq t} \sum_{k \in K_L} x_{akv}^L \quad \forall a \in \Omega_L, t \quad (30)$$

$$\sum_{a \in \Omega_i^+} y_{at}^{L+} + \sum_{a \in \Omega_i^-} y_{at}^{L-} = 1 \quad \forall i \in \Omega_{PL}, t \quad (31)$$

$$\sum_{a \in \Omega_i^+} y_{at}^{L+} + \sum_{a \in \Omega_i^-} y_{at}^{L-} = 0 \quad \forall i \in \Omega_{SS}, t \quad (32)$$

$$\sum_{a \in \Omega_i^+} f_{at}^L - \sum_{a \in \Omega_i^-} f_{at}^L = f_{it}^{PL} - f_{it}^{SS} \quad \forall i \in \Omega_{PN}, t \quad (33)$$

$$-|\Omega_{PL}|(y_{at}^{L+} + y_{at}^{L-}) \leq f_{at}^L \leq |\Omega_{PL}|(y_{at}^{L+} + y_{at}^{L-}) \quad \forall a \in \Omega_L, t \quad (34)$$

$$f_{it}^{PL} = \begin{cases} 1 & \forall i \in \Omega_{PL} \\ 0 & \forall i \notin \Omega_{PL}, \forall t \end{cases} \quad (35)$$

$$0 \leq f_{it}^{SS} \leq |\Omega_{PL}| \quad \forall i \in \Omega_{SS}, \forall t \quad (36)$$

To illustrate the operational constraints for HES, the energy flow in the HES [21] is presented in Fig. 2. Specifically, the HGSs produce the hydrogen and compress it to a certain pressure for HT transportation or storage in the HSs. As for HT, it can transport the hydrogen to HRSs and return to the HGSs when the loading hydrogen is empty. Both the HGSs and HRSs are equipped with HSs to increase operational flexibility.

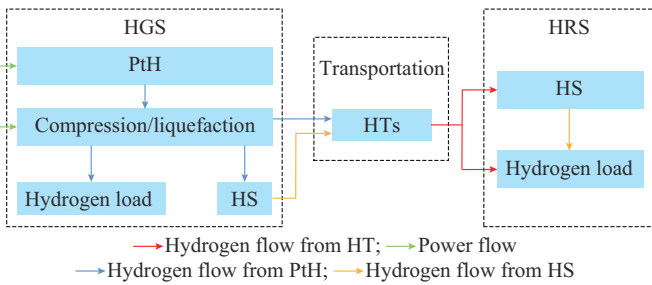


Fig. 2. Energy flow in HES.

3) Hydrogen production constraints: constraint (37) defines that the hydrogen productions from PtHs are exported to the HTs, stored in the HS, or provided to the local hydrogen load. Constraint (38) presents the hydrogen balance of HSs within HGSs. Constraint (39) defines the hydrogen export balance from HGS to the HTs. Constraints (40)-(42) present the capacity and operation boundaries of HSs within HGSs. Constraint (43) indicates the exported hydrogen limits of PtHs.

$$\sum_{\tau \in \tau'} h_{gst\tau'}^{PtH} = h_{gst\tau'}^{ex} + h_{gst\tau'}^{ch} + \sum_{\tau \in \tau'} (h_{gst\tau}^D - h_{gst\tau}^{CD}) \quad \forall g \in \Omega_{PtH}, t, s, \tau' \quad (37)$$

$$E_{gst\tau'}^{HGS} = E_{gst, \tau'-1}^{HGS} + h_{gst\tau'}^{ch} - h_{gst\tau'}^{dis} \quad \forall g \in \Omega_{PtH}, t, s, \tau' \quad (38)$$

$$h_{gst\tau'}^{ex} + h_{gst\tau'}^{dis} = \sum_{d \in \Omega_{HT}^g} h_{gst\tau'}^{toHT, d} \quad \forall g \in \Omega_{PtH}, t, s, \tau' \quad (39)$$

$$E_{gst, 0}^{HGS} = E_{gst, N\tau'}^{HGS} = x_{gt}^{HS} / 2 \quad \forall g \in \Omega_{PtH}, t, s, \tau' \quad (40)$$

$$x_{gt}^{HS} \underline{\delta} \leq E_{gst\tau'}^{HGS} \leq x_{gt}^{HS} \bar{\delta} \quad \forall g \in \Omega_{PtH}, t, s, \tau' \quad (41)$$

$$\begin{cases} 0 \leq h_{gst\tau'}^{ch} \leq x_{gt}^{HS} \mu_{HS} \Delta_{\tau'} \\ 0 \leq h_{gst\tau'}^{dis} \leq x_{gt}^{HS} \mu_{HS} \Delta_{\tau'} \end{cases} \quad \forall g \in \Omega_{PtH}, t, s, \tau' \quad (42)$$

$$0 \leq h_{gst\tau'}^{ex} \leq x_{gt}^{PtH} \mu_{ex} \Delta_{\tau'} \quad \forall g \in \Omega_{PtH}, t, s, \tau' \quad (43)$$

4) Hydrogen transportation constraints: the HT-based hydrogen transportation process is modeled as a vehicle routing problem [7], [8] as in (44)-(48). Constraints (44) and (45) restrict that the HTs will depart from a certain HGS and arrive at an HRS after leaving the HGS. Constraint (46) ensures that the HTs will return to the original HGS at the end of the transportation process. Constraint (47) indicates that the HTs will leave from one HRS to another HRS after providing hydrogen. Constraint (48) introduces an auxiliary variable $\beta_{dst\tau'}^m$ for each HT and restricts it to increase along the transportation trip. It guarantees that the HTs will not return to the visited HRS within each transportation trip, and the closed loops among HRSs can be avoided [7]. Constraint (49) presents the hydrogen import balance from an HT to the HRSs. The upper bound of hydrogen transferred from the HGS to an HT is restricted by (50), and the hydrogen imported from HTs to the HRSs is constrained by (51).

$$\sum_{m \in \Omega_{HT}} \sum_{n \in \Omega_{HT}} \alpha_{dst\tau'}^{m, n} \leq M \sum_{m \in \Omega_{HT}} \alpha_{dst\tau'}^{g, m} \quad \forall g \in \Omega_{PtH}, d \in \Omega_{HT}^g, t, s, \tau' \quad (44)$$

$$\sum_{m \in \Omega_{HT}} \alpha_{dst\tau'}^{g, m} \leq 1 \quad \forall g \in \Omega_{PtH}, d \in \Omega_{HT}^g, t, s, \tau' \quad (45)$$

$$\sum_{m \in \Omega_{HT}} \alpha_{dst\tau'}^{g, m} = \sum_{m \in \Omega_{HT}} \alpha_{dst\tau'}^{m, g} \quad \forall g \in \Omega_{PtH}, d \in \Omega_{HT}^g, t, s, \tau' \quad (46)$$

$$\sum_{n \in \Omega_{HT}} \alpha_{dst\tau'}^{m, n} = \sum_{n \in \Omega_{HT}} \alpha_{dst\tau'}^{n, m} \quad \forall m \in \Omega_{HT}, d, t, s, \tau' \quad (47)$$

$$\beta_{dst\tau'}^m - \beta_{dst\tau'}^n + |\Omega_{HT}| \alpha_{dst\tau'}^{m, n} \leq |\Omega_{HT}| - 1 \quad \forall m, n \in \Omega_{HT}, d, t, s, \tau' \quad (48)$$

$$h_{gst\tau'}^{toHT, d} = \sum_{m \in \Omega_{HT}} h_{mst\tau'}^{im, d} \quad \forall g \in \Omega_{PtH}, d \in \Omega_{HT}^g, t, s, \tau' \quad (49)$$

$$0 \leq h_{gst\tau'}^{toHT, d} \leq \bar{H}_{in}^{HT} \sum_{m \in \Omega_{HT}} \alpha_{dst\tau'}^{g, m} \quad \forall g \in \Omega_{PtH}, d \in \Omega_{HT}^g, t, s, \tau' \quad (50)$$

$$0 \leq h_{mst\tau'}^{im, d} \leq \bar{H}_{out}^{HT} \sum_{n \in \Omega_{HT}} \alpha_{dst\tau'}^{n, m} \quad \forall m \in \Omega_{HT}, d, t, s, \tau' \quad (51)$$

5) Hydrogen refueling station constraints: constraint (52) indicates the hydrogen balance of HSs within HRSs. Constraints (53) and (54) represent the operation boundaries of HSs within HRSs. Hydrogen load and the maximum curtailed hydrogen load at each HRS are restricted in (55).

$$E_{mst\tau'}^{HRS} = E_{mst, \tau'-1}^{HRS} + \sum_{d \in \Omega_{HT}} h_{mst\tau'}^{im, d} - \sum_{\tau \in \tau'} (h_{mst\tau}^D - h_{mst\tau}^{CD}) \quad \forall m \in \Omega_{HT}, t, s, \tau' \quad (52)$$

$$E_{mst, 0}^{HRS} = E_{mst, N\tau'}^{HRS} = x_{mt}^{HS} / 2 \quad \forall m \in \Omega_{HT}, t, s, \tau' \quad (53)$$

$$x_{mt}^{\text{HS}} \underline{\delta} \leq E_{mst}^{\text{HRS}} \leq x_{mt}^{\text{HS}} \bar{\delta} \quad \forall m \in \Omega_{\text{HL}}, t, s, \tau \quad (54)$$

$$\begin{cases} h_{mst}^{\text{D}} = \zeta_{st}^{\text{HL}} H_{mt}^{\text{D}} \\ 0 \leq h_{mst}^{\text{CD}} \leq \zeta_{\text{CH}} h_{mst}^{\text{D}} \end{cases} \quad \forall m \in \Omega_{\text{HL}}, t, s, \tau \quad (55)$$

6) Coupling constraints: the PDS is coupled with HES through the PtHs. The power consumed by the PtHs and the compressors is shown in (56) and (57), respectively.

$$h_{gts}^{\text{PtH}} = \eta_{\text{PtH}} p_{gst}^{\text{PtH}} \Delta_{\tau} \quad \forall g \in \Omega_{\text{PtH}}, t, s, \tau \quad (56)$$

$$p_{gst}^{\text{Com}} \Delta_{\tau} = \eta_{\text{Com}} h_{gts}^{\text{PtH}} \quad \forall g \in \Omega_{\text{PtH}}, t, s, \tau \quad (57)$$

The overall planning model is an MISOCP problem with objective (1) and subject to constraints (7)-(57).

IV. SOLVING ALGORITHM

In this section, the original MISOCP model is firstly converted into an MILP problem to relieve the computation burden by linearizing the second-order cone constraints. Then, a multi-stage stochastic MILP model is formulated to address the long-term power/hydrogen growth uncertainties.

A. Linearization of Nonlinear Constraints

In the original MISOCP model, (17) and (18) are second-order cone constraints. A polyhedral approximation method [26] is introduced to linearize them. For (17) and (18), they can be transformed into a general form of second-order cone constraint, as in (58). Note that (18) is a rotated conic quadratic constraint, the transformation process from (18) to (58) can be observed in [27]. A set of linear constraints associated with a number of auxiliary variables $(\kappa_0, \kappa_1, \dots, \kappa_{N_v})$ and $(\vartheta_0, \vartheta_1, \dots, \vartheta_{N_v})$ to approximate (58), as in (59). The linearization error will decrease as the N_v increases (N_v is set to be 4 in this paper).

$$\sqrt{z_1^2 + z_2^2} \leq z_3 \quad (58)$$

$$\begin{cases} \kappa_0 \geq |z_1| \\ \vartheta_0 \geq |z_2| \\ \kappa_v = \kappa_{v-1} \cos\left(\frac{\pi}{2^{v+1}}\right) + \vartheta_{v-1} \sin\left(\frac{\pi}{2^{v+1}}\right) \quad \forall v = 1, 2, \dots, N_v \\ \vartheta_v \geq \left| -\kappa_{v-1} \sin\left(\frac{\pi}{2^{v+1}}\right) + \vartheta_{v-1} \cos\left(\frac{\pi}{2^{v+1}}\right) \right| \quad \forall v = 1, 2, \dots, N_v \\ \kappa_{N_v} \leq z_3 \\ \vartheta_{N_v} \leq \kappa_{N_v} \tan\left(\frac{\pi}{2^{N_v+1}}\right) \end{cases} \quad (59)$$

In general, the mathematical formulation for the proposed planning model can be written as a compact MILP model with the investment variables $\mathbf{x}_1, \mathbf{x}_2, \dots, \mathbf{x}_{|\Omega_t|}$ and the operational variables $\mathbf{y}_1, \mathbf{y}_2, \dots, \mathbf{y}_{|\Omega_t|}$ as follows.

$$\min_{\{\mathbf{x}_t, \mathbf{y}_t\}} \sum_{t \in \Omega_t} f_t(\mathbf{x}_t, \mathbf{y}_t) \quad (60)$$

s.t.

$$\mathbf{B}_t \mathbf{x}_{t-1} + \mathbf{A}_t \mathbf{x}_t \leq \mathbf{e}_t \quad \forall t \in \Omega_t \quad (61)$$

$$\mathbf{C}_t \mathbf{x}_t + \mathbf{D}_t \mathbf{y}_t \leq \mathbf{h}_t \quad \forall t \in \Omega_t \quad (62)$$

where $\mathbf{A}_t, \mathbf{B}_t, \mathbf{C}_t, \mathbf{D}_t, \mathbf{e}_t$, and \mathbf{h}_t are the coefficient matrices; and \mathbf{x}_t is the investment decision. Equation (60) corresponds

to (1), (61) corresponds to (7)-(13), and (62) corresponds to (14)-(16), (19)-(57), and (59).

B. Multi-stage Stochastic Programming with Non-anticipativity Constraints

In practical engineering, the long-term IPDHS co-planning problem will face load growth uncertainties during the planning horizon [11], [28]. To address this problem, a multi-stage stochastic model with non-anticipativity constraints [29], [30] is utilized in this paper to obtain flexible investment decisions to resist long-term uncertainties.

A scenario tree is developed to characterize the load growth uncertainties and describe possible sequential decisions over planning horizons, as shown in Fig. 3, where $x_{t,c}$ is the investment decision of scenario c at stage t . Detailed modeling for a scenario tree can be found in [31]. The root node represents the power/hydrogen load state at the first stage. The branch arcs from the root to the leaves $(\omega_{1,c}, \omega_{2,c}, \dots, \omega_{|\Omega_t|,c})$ construct a scenario ξ_c , in which $\omega_{t,c}$ represents the uncertain realization of load growth state at each stage.

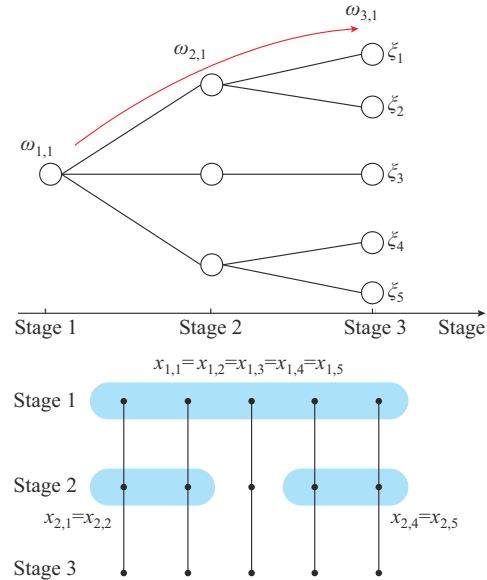


Fig. 3. Scenario tree and sequential decisions with non-anticipativity.

Traditionally, a two-stage stochastic model [30] can be utilized to address load growth uncertainties, which can be formulated as in (63)-(65).

$$\min_{\{\mathbf{x}_t, \mathbf{y}_t\}} \sum_{t \in \Omega_t} \left(\mathbf{c}^T \mathbf{x}_t + \sum_{c \in \Omega_c} p_{t,c} f_t(\mathbf{x}_t, \mathbf{y}_{t,c}(\omega_{t,c})) \right) \quad (63)$$

s.t.

$$\mathbf{B}_t \mathbf{x}_{t-1} + \mathbf{A}_t \mathbf{x}_t \leq \mathbf{e}_t \quad \forall t \in \Omega_t \quad (64)$$

$$\mathbf{C}_t \mathbf{x}_t + \mathbf{D}_t \mathbf{y}_{t,c}(\omega_{t,c}) \leq \mathbf{h}_t(\omega_{t,c}) \quad \forall t \in \Omega_t \quad (65)$$

The investment decision \mathbf{x}_t is the first-stage variable, and the operation decisions $\mathbf{y}_{t,c}(\omega_{t,c})$ are the second-stage variables. In this framework, \mathbf{x}_t is determined before the uncertainties are realized, while $\mathbf{y}_{t,c}(\omega_{t,c})$ are made according to different realizations of $\omega_{t,c}$. The main disadvantage is that the investment decisions cannot be changed during the multi-stage planning process, which sacrifices the flexibility of the decision-making.

To enable a set of flexible decisions in each scenario for both investment and operation variables, a multi-stage stochastic MILP model is formulated as follows.

$$\min \sum_{\{x,y\}} \sum_{t \in \Omega_t, c \in \Omega_c} p_{t,c} [c^T x_{t,c}(\omega_{t,c}) + d^T y_{t,c}(\omega_{t,c})] \quad (66)$$

s.t.

$$B_t x_{t-1,c}(\omega_{t-1,c}) + A_t x_{t,c}(\omega_{t,c}) \leq e_t \quad \forall t \in \Omega_t \quad (67)$$

$$C_t x_{t,c}(\omega_{t,c}) + D_t y_{t,c}(\omega_{t,c}) \leq h_t \quad \forall t \in \Omega_t \quad (68)$$

$$x_{t,c}(\omega_{t,c}) = x_{t,c'}(\omega_{t,c'})$$

$$\forall c, c' \in \Omega_c \cap \{\omega_{1,c}, \omega_{1,c'}, \dots, \omega_{t-1,c}, \omega_{t-1,c'}\} = \{\omega_{1,c'}, \omega_{1,c'}, \dots, \omega_{t-1,c'}\} \quad (69)$$

where the investment decisions $x_{t,c}(\omega_{t,c})$ are adjustable to the future realization of load growth uncertainties $\omega_{t,c}$. Equation (69) is a non-anticipativity constraint [30], and it ensures that the investment decisions corresponding to scenarios with the same load growth state at stage t should be equal, as shown in Fig. 3.

Compared with the two-stage stochastic model in (63)-(65) which obtains a determined planning decision over the planning horizons, the multi-stage stochastic model in (66)-(69) can obtain a more flexible decision tree. As the uncertain load growth state is revealed gradually over stages, the planners can choose planning decisions based on the latest information.

V. CASE STUDY

A. Initial Parameters and Data

The proposed IPDHS co-planning model is tested on three systems [20], [24], [32]. Firstly, it is tested on a modified 8-node PDS with a 7-node HES, with several analyses for the planning results. To validate its scalability, a modified 24-node PDS with a 9-node HES system, and a modified 54-node PDS with a 9-node HES system, are subsequently performed. The planning horizon is assumed to be 15 years subdivided into 3 stages of 5 years. The interest rate is set to be 8%. Three typical days in summer, winter, and transition seasons are utilized to represent the stochastic nature of PVs, WTs, power load, hydrogen load, and electricity price, as shown in Fig. 4. All the cases are modeled in YALMIP solved by GUROBI in MATLAB R2021a.

Figure 5 shows the topology of the 8-node PDS with a 7-node hydrogen transportation system. It consists of 1 substation (35 kV), 7 power load nodes, 2 existing power lines, 7 candidate power lines, 2 HGSSs, 5 HRSs, and 9 roads.

The forecast power and hydrogen load of 8-node PDS are presented in Table I.

Table II presents the uncertain load growth state and probability at each stage. Candidate power lines and transformer data for 8-node PDS are shown in Tables III and IV. The PV and WT data for 8-node PDS are given in Table V. In the HES, nodes 6 and 7 in the HGS are connected to nodes 1 and 2 in the PDS, respectively. Each HGS is equipped with two HTs for hydrogen transportation. Three time periods ($N_{\tau}=3$, $\Delta_{\tau}=8$ hours) are considered for HTs in each day. The HES parameters are presented in Table VI. More data related to the test system can refer to [33]. The optimality gap is set to be 0.5% for this case, and the proposed model needs 0.7 hour to find the optimal decision.

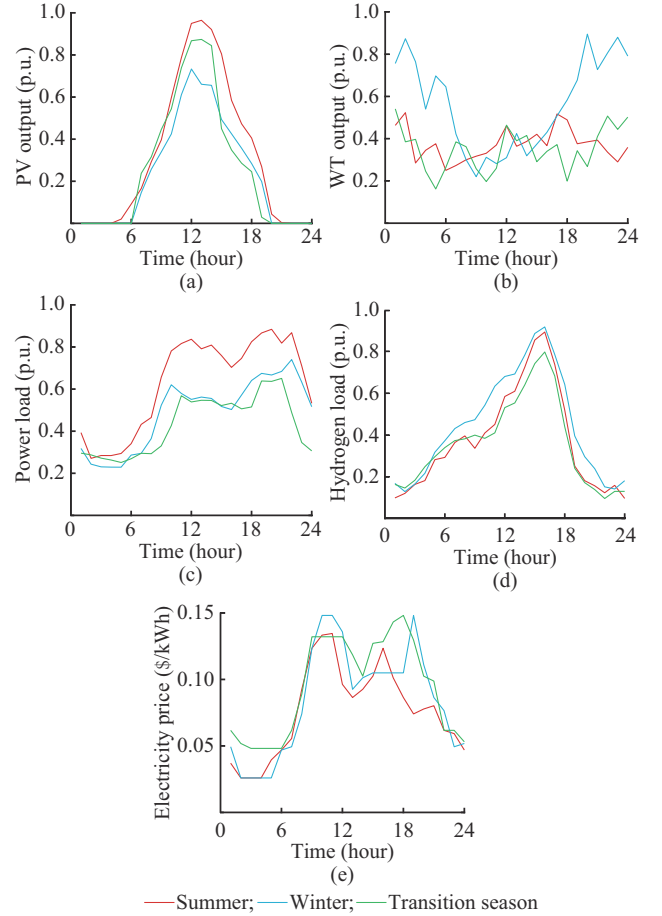


Fig. 4. Three typical days in summer, winter, and transition season representing stochastic nature of PVs, WTs, power load, hydrogen load, and electricity price. (a) PV. (b) WT. (c) Power load. (d) Hydrogen load. (e) Electricity price.

In order to illustrate the effectiveness of the proposed multi-stage stochastic IPDHS co-planning model, five cases are designed and compared.

Case 1: the proposed multi-stage stochastic IPDHS co-planning model.

Case 2: this case is a two-stage stochastic IPDHS co-planning model as in (61)-(63).

Case 3: the multi-stage planning framework is utilized. The PDS expansion and PtHs are firstly optimized, after which the HES capacity is optimized (including hydrogen transportation and HSs).

Case 4: the multi-stage planning framework is utilized. The HES capacity is firstly optimized (including PtHs, hydrogen transportation and HSs), after which the PDS expansion is deployed.

Case 5: this case is similar to Case 1, while the spatial distribution of hydrogen load is varied as listed in Table I.

Table VII presents the cost comparison of five cases. Case 1 and Case 2 are compared to investigate the influence of the multi-stage planning model. It can be observed that the investment costs and the total planning costs of Case 1 are lower than those of Case 2, which shows the merits of multi-stage planning in dealing with long-term load growth uncertainties.

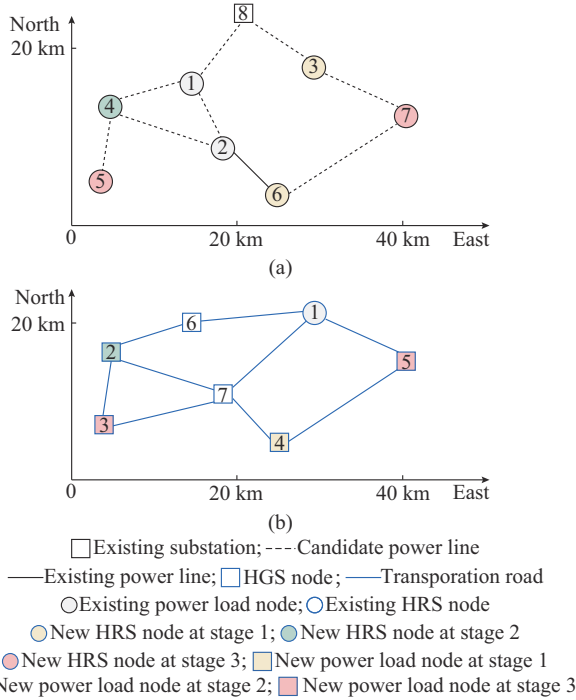


Fig. 5. Topology of 8-node PDS with a 7-node hydrogen transportation system. (a) Under 8-node PDS. (b) Under 7-node hydrogen transportation system.

TABLE I
FORECAST POWER AND HYDROGEN LOAD OF 8-NODE PDS

Scenario	Power node	Power load (MVA)	Hydrogen node	Hydrogen load (kg)	
				Cases 1-4	Case 5
Stages 1, 2, 3	1	4.05, 4.58, 4.74	1	16, 20, 24	8, 12, 16
	2	1.14, 1.50, 1.76	4	12, 20, 24	24, 24, 32
	3	0.78, 1.50, 1.80	6	20, 24, 28	12, 16, 16
	6	0.32, 1.00, 1.60	7	12, 16, 24	16, 24, 28
Stages 2, 3	4	2.05, 2.30	2	16, 28	20, 24
Stage 3	5	1.22	3	12	20
	7	1.68	5	8	12

TABLE II
UNCERTAIN LOAD GROWTH STATE AND PROBABILITY AT EACH STAGE

Scenario	x (y)		
	Stage 1	Stage 2	Stage 3
ξ_1		0.9 (30%)	0.9 (50%)
ξ_2			1.0 (50%)
ξ_3	1.0 (100%)	1.0 (40%)	1.0 (100%)
ξ_4			1.15 (70%)
ξ_5		1.15 (30%)	0.95 (30%)

Note: x and y in $x(y)$ represent the load growth state and the probability, respectively.

To further illustrate it, planning decisions in Case 1 and Case 2 are given in Table VIII. In Case 1, all the scenarios get the same planning results at stage 1. At stage 2, there are

three candidate planning decisions for planners to choose from, which correspond to different load growth states. Similarly, there are five choices to be selected at stage 3. However, in Case 2, only one investment decision can be obtained, and the operation variables can be adjusted to cope with different load growth states. Therefore, the planning decision-making process in Case 1 is more flexible than that in Case 2, which can be adjusted according to the future load growth information.

TABLE III
CANDIDATE POWER LINES FOR 8-NODE PDS

Type	Resistance (Ω/km)	Reactance (Ω/km)	Capacity (MVA)	Cost ($\$/\text{km}$)
1	0.614	0.399	9.38	28020
2	0.507	0.480	12.80	35140

TABLE IV
TRANSFORMER DATA FOR 8-NODE PDS

Type	Capacity (MVA)	Investment ($\$$)	Maintenance ($\$$)
1	10	400000	2000
2	15	580000	3000

TABLE V
PV AND WT DATA FOR 8-NODE PDS

Type	Investment for stages 1, 2, 3 ($\$/\text{MW}$)	Maintenance cost ($\$/\text{kW}$)	Operation cost ($\$/\text{kWh}$)	Curtailement cost ($\$/\text{kWh}$)
PV	1.7, 1.6, 1.5	4% of investment cost	0.01	0.2
WT	1.3, 1.2, 1.1		0.01	0.2

TABLE VI
PARAMETERS FOR HES

Parameter	Value
λ_1^{Tr} ($\$/\text{km}$)	1.3
λ_2^{Tr} ($\$/\text{km}$)	0.7
λ_3^{Tr} ($\$/\text{km}$)	1.3
λ_d^{Dis} ($\$$ per HT)	100
μ_{HS}	0.5
μ_{ex}	1.0
$\delta, \bar{\delta}$	0.1, 0.9
$\bar{H}_{\text{in}}^{\text{HT}}, \bar{H}_{\text{out}}^{\text{HT}}$ (kg)	300, 300
η_{PH} (kg/kWh)	52
η_{com} (kWh/kg)	1.0
C^{LPH} ($\$/\text{MW}$)	1.40 (stage 1), 1.30 (stage 2), 1.20 (stage 3)
C^{LHS} ($\$/\text{kg}$)	20

Cases 1, 3, and 4 are considered for comparison to show the effect of coordinated planning of PDS and HES. Clearly, Case 1 optimizes the IPDHS in a coordinated way and features the lowest total costs among them. In Case 3, the PDS planning is initially optimized, which obtains lower PDS ex-

pansion costs and leads to higher planning costs for HES. In contrast, Case 4 firstly optimizes the HES and achieves the cheapest HES planning costs, while the PDS expansion costs increase.

TABLE VII
COST COMPARISON OF FIVE CASES

System	Type	Cost (\$10 ⁵)				
		Case 1	Case 2	Case 3	Case 4	Case 5
PDS	Investment	6.52	6.78	6.53	6.60	6.52
	Maintenance	3.40	3.47	3.41	3.45	3.40
	Production	91.16	91.08	90.61	92.50	90.82
	Curtailement	0.54	0.59	0.57	0.85	0.54
	Total	101.62	101.92	101.12	103.40	101.28
HES	Investment	7.25	7.31	8.49	5.85	7.45
	Maintenance	4.49	4.50	5.30	3.52	4.53
	Production	23.67	23.72	22.65	24.96	23.28
	Curtailement	0	0	0	0	0
	Total	35.41	35.53	36.44	34.33	35.26
IPDHS	Total	137.03	137.45	137.56	137.73	136.54

TABLE VIII
PLANNING DECISIONS OF 8-NODE PDS IN CASE 1 AND CASE 2

Case	Scenario (probability)	Planning decision		
		Stage 1	Stage 2	Stage 3
Case 1	Scenario 1 (0.15)		Power line: 1-4(2); WT: 2(0.75), 3(0.75), 6(1.10); PtH: 6 (2.85), 7 (1.85); HS: 1 (400.0), 2 (478.8), 3 (143.9), 4 (341.0), 6 (426.3)	Power line: 3-7(1), 4-5(1), 6-7(1); substation: 8(1); PV: 7(1.19); WT: 2(0.80), 3(1.10), 6(1.55); PtH: 6 (2.55), 7 (3.56); HS: 1 (434.4), 2 (600.0), 3 (172.7), 4 (502.3), 5 (238.7), 6 (511.5), 7 (57.6)
	Scenario 2 (0.15)		Power line: 3-7(1), 4-5(1), 6-7(1); substation: 8(1); PV: 7(1.39); WT: 2(0.80), 3(1.10), 6(1.80); PtH: 6 (2.85), 7 (3.14); HS: 1 (600.0), 2 (580.4), 3 (430.6), 4 (471.2), 5 (86.4), 6 (426.3), 7 (57.6)	
	Scenario 3 (0.40)	Power line: 2-6(2), 3-8(2); WT: 2(0.16), 3(0.75), 6(0.80); PtH: 6 (1.53), 7 (1.11); HS: 1 (400.0), 2 (304.6), 3 (115.1), 6 (86.4)	Power line: 1-4(2), 3-7(2), 6-7(1); PV: 4(0.56), 7(0.56); WT: 2(0.74), 3(0.82), 6(1.10); PtH: 6 (2.89), 7 (1.85); HS: 1 (453.8), 2 (478.8), 3 (143.9), 4 (287.0), 6 (143.9)	Power line: 4-5(1); substation: 8(1); PV: 4(0.56), 7(0.83); WT: 2(0.80), 3(1.10), 6(1.80); PtH: 6 (3.16), 7 (2.80); HS: 1 (600.0), 2 (478.8), 3 (430.6), 4 (316.8), 5 (238.7), 6 (172.7), 7 (57.6)
	Scenario 4 (0.21)		Power line: 1-4(2), 3-7(2), 6-7(2); PV: 4(0.56), 7(0.56); WT: 2(0.74), 3(1.07), 6(1.20); PtH: 6 (3.06), 7 (1.76); HS: 1 (456.2), 2 (456.2), 3 (346.7), 4 (341.0), 6 (426.3)	Power line: 4-5(2); substation: 8(1); PV: 4(0.66), 7(1.18); WT: 2(0.80), 3(1.20), 6(1.80); PtH: 6 (3.06), 7 (3.34); HS: 1 (600.0), 2 (600.0), 3 (430.6), 4 (341.0), 5 (255.8), 6 (511.5), 7 (57.6)
	Scenario 5 (0.09)			Power line: 4-5(2); substation: 8(1); PV: 4(0.66), 7(0.66); WT: 2(0.80), 3(1.20), 6(1.51); PtH: 6 (3.63), 7 (2.46); HS: 1 (456.2), 2 (456.2), 3 (511.5), 4 (460.4), 5 (197.3), 6 (426.3), 7 (57.6)
Case 2		Power line: 2-6(2), 3-8(2); WT: 2(0.45), 3(0.45), 6(0.80); PtH: 6 (1.53), 7 (1.11); HS: 1 (400.0), 2 (315.4), 3 (115.1), 6 (238.7)	Power line: 1-4(2), 3-7(2), 6-7(2); substation: 8(1) PV: 4(0.66), 7(0.66); WT: 2(0.45), 3(1.06), 6(1.08); PtH: 6 (2.97), 7 (1.85); HS: 1 (500.0), 2 (490.3), 3 (358.8), 4 (341.0), 6 (358.8)	Power line: 4-5(2); PV: 4(0.58), 7(0.76); WT: 2(0.80), 3(1.08), 6(1.80); PtH: 6 (3.17), 7 (2.79); HS: 1 (500.0), 2 (600.0), 3 (511.5), 4 (502.3), 5 (255.8), 6 (511.5), 7 (70.5)

Note: planning decisions are presented as $x(y)$. For power lines, x and y refer to the line mark and conductor type, respectively. For PV (MW), WT (MW), PtH (MW) and HS (kg), x and y refer to the node mark and installed capacity, respectively. Non-bold nodes and bold nodes represent the PDS and HES nodes, respectively.

Moreover, it can be found that the RES curtailment costs in Case 1 are lower than those in Case 3 and Case 4, which means that the RES utilization rate can be enhanced through coordinated planning.

As the interface between PDS and HES, the capacity allocation of PtHs will influence the planning results of both systems. Among Case 1, Case 3, and Case 4, Case 1 provides a tradeoff between PDS and HES, which can improve the RES

consumption rate and achieve the highest economic benefits.

Furthermore, Case 1 and Case 5 are compared to show the influence of hydrogen load spatial distribution on the planning results. It can be observed that the planning costs of PDS and HES are both changed. The reason is that the variations in nodal hydrogen load will influence the transportation process from the HGS to the HRSs, and thus change the PtH allocations and the overall planning decisions.

For further illustration, the planning results for the PDS network in Case 1 in scenario ζ_5 are presented in Fig. 6, where the operation power lines are bold in black. The PDS network structure at each stage can be operated in radiality. Furthermore, Table IX presents the transportation route for HTs in Case 1 in scenario ζ_5 . In one day, there are three scheduling periods for HTs to take away the produced hydrogen from HGS to the HRS. As can be observed, HTs 1-4 can coordinate together to complete the hydrogen transportation task effectively.

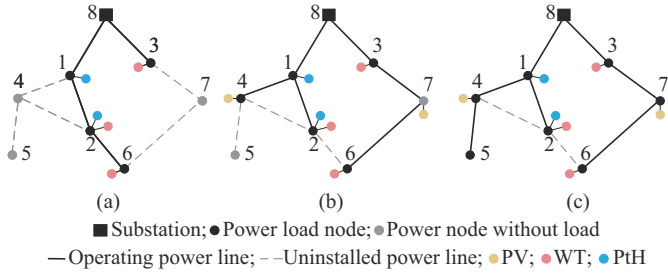
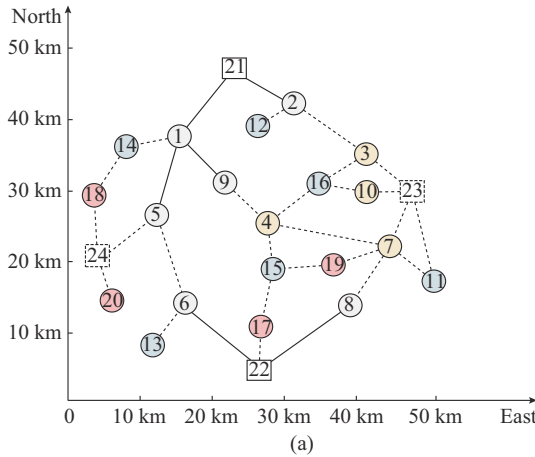


Fig. 6. Planning results for PDS in Case 1 in scenario ζ_5 , (a) Stage 1. (b) Stage 2. (c) Stage 3.



□ HGS node; □ Existing substation; □ Uninstalled substation; --- Candidate power line; — Existing power line; — Transportation road
○ Existing power load node; ○ Existing HRS node; ○ New HRS node at stage 1; ○ New HRS node at stage 2; ○ New HRS node at stage 3
■ New power load node at stage 1; ■ New power load node at stage 2; ■ New power load node at stage 3

Fig. 7. Initial topology. (a) Under 24-node PDS. (b) Under 9-node HES.

Table X presents the uncertain load growth state and probability at each stage in the 24-node PDS. The optimality gap in this system is set as 1.0%, and the computation time is 9.69 hours.

TABLE X
UNCERTAIN LOAD GROWTH STATE AND PROBABILITY AT EACH STAGE FOR
24-NODE PDS AND 9-NODE HES

Scenario	$x(y)$		
	Stage 1	Stage 2	Stage 3
ζ_1		0.9 (20%)	0.9 (20%)
ζ_3	1.0 (100%)	1.0 (50%)	1.0 (50%)
ζ_5		1.15 (30%)	1.15 (30%)

Note: x and y in $x(y)$ represent the load growth state and the probability, respectively.

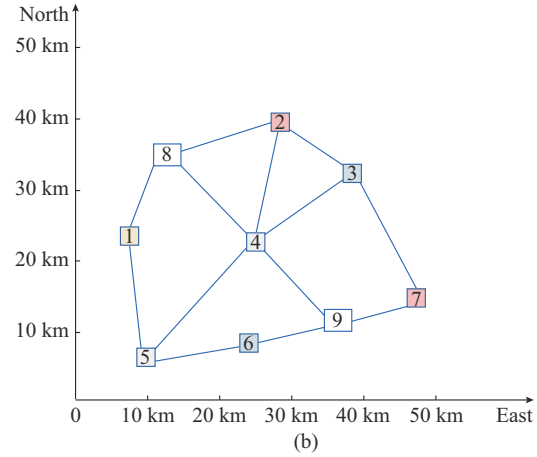
TABLE IX
TRANSPORTATION ROUTE FOR HTs IN CASE 1 IN SCENARIO ζ_5

No.	Transportation route of HTs at each stage		
	Stage 1	Stage 2	Stage 3
HT1		6-2-6-2-6-1-6	6-2-3-6-2-6-2-3-6
HT2		6-6-6-2-6	6-6-1-6-2-6
HT3	7-4-7-4-7-4-7	7-4-7-4-7-4-7	7-4-7-1-5-7-4-7
HT4	7-1-7-1-7-1-7	7-1-7-1-7-1-7	7-1-5-7-4-7-1-7

Note: non-bold nodes and bold nodes represent the PDS and HES nodes, respectively.

B. 24-node PDS

To validate the scalability of the planning method, a modified 24-node PDS with a 9-node HES is applied. The initial topology is shown in Fig. 7. The PDS comprises 4 substations (35 kV), 20 power load nodes, 6 existing power lines, 25 candidate power lines, 2 HGSs, 7 HRSs, and 13 roads. In the HES, two HGS nodes 8 and 9 are connected to nodes 1 and 8 in the PDS, respectively.



The cost comparison of five cases in the 24-node PDS is presented in Table XI, and the planning decisions of 24-node PDS in Case 1 and Case 2 are presented in Table XII. In the 24-node PDS, similar conclusions can be obtained as in the 8-node PDS. The proposed planning model considers the coordination of PDS and HES, and the investment decisions are determined from a holistic perspective. Two test systems both verify that the planning method provides a tradeoff between the PDS and the HES, which can reduce the total planning cost and promote RES utilization. Besides, the multi-stage stochastic planning model outperforms the two-stage stochastic model, which can provide a decision tree for planners under power and hydrogen load growth uncertainties and make the decision-making process more flexible.

TABLE XI
COST COMPARISON OF FIVE CASES FOR 24-NODE PDS AND 9-NODE HES

System	Type	Cost (\$10 ⁵)				
		Case 1	Case 2	Case 3	Case 4	Case 5
PDS	Investment	18.53	18.14	18.24	18.70	18.53
	Maintenance	8.89	8.67	8.77	8.93	8.89
	Production	181.30	182.51	181.04	184.66	181.12
	Curtailement	1.42	1.47	1.48	1.75	1.42
	Total	210.14	210.79	209.53	214.04	209.96
HES	Investment	15.36	15.19	16.06	14.20	15.44
	Maintenance	9.38	9.35	9.85	8.71	9.61
	Production	34.39	34.89	34.48	35.65	34.59
	Curtailement	0	0	0	0	0
	Total	59.13	59.43	60.39	58.56	59.64
IPDHS	Total	269.27	270.22	269.92	272.60	269.60

TABLE XII
PLANNING DECISIONS OF 24-NODE PDS IN CASE 1 AND CASE 2

Case	Scenario (probability)	Planning decision		
		Stage 1	Stage 2	Stage 3
Case 1	Scenario 1 (0.2)	Power line: 4-9, 3-16, 3-23, 7-23, 10-23; substation: 23;	Power line: 1-14, 2-12, 6-13, 11-23, 15-17, 17-22; PV: 1(0.44), 4(0.88), 15(0.86); WT: 2(2.50), 9(2.50), 14(0.27); PtH: 8 (4.46), 9 (6.00); HS: 1 (574.1), 3 (172.7), 4 (287.9), 5 (184.7), 6 (688.9), 8 (1500.0), 9 (1500.0)	Power line: 5-24, 7-19, 10-16, 18-24, 20-24; substation: 24; PV: 1(0.44), 4(2.12), 15(0.86); WT: 2(3.50), 9(3.50), 14(1.30), 18(0.79); PtH: 8 (6.12), 9 (6.28); HS: 1 (574.1), 2 (230.3), 3 (207.3), 4 (322.4), 5 (209.0), 6 (688.9), 7 (172.7), 8 (1500.0), 9 (2000.0)
	Scenario 1 (0.5)	PV: 1(0.35), 4(0.86); WT: 2(1.50), 9(1.43); PtH: 8 (3.25), 9 (1.64); HS: 1 (574.1), 4 (230.3), 5 (172.7), 8 (1000.0), 9 (630.3)	Power line: 1-14, 2-12, 6-13, 10-16, 11-23, 15-17, 17-22; PV: 1(0.35), 4(1.22), 15(0.85); WT: 2(2.50), 9(2.50), 14(0.86); PtH: 8 (4.62), 9 (6.00); HS: 1 (1023.0), 3 (172.7), 4 (287.9), 5 (230.3), 6 (286.1), 8 (1425.6), 9 (1500.0)	Power line: 2-3, 5-24, 7-19, 18-24, 20-24; substation: 24; PV: 1(0.35), 4(2.71), 15(0.85); WT: 2(3.50), 9(3.50), 14(1.21), 18(1.31), 20(0.39); PtH: 8 (6.22), 9 (6.61); HS: 1 (1023.0), 2 (230.3), 3 (207.3), 4 (322.4), 5 (264.8), 6 (481.1), 7 (172.7), 8 (2000.0), 9 (2000.0)
	Scenario 1 (0.3)	Power line: 4-9, 3-23, 7-23, 10-23; PV: 1(0.35), 4(0.87); WT: 2(1.50), 9(1.43); PtH: 8 (2.10), 9 (2.86); HS: 1 (526.2), 4 (230.3), 5 (477.3), 8 (705.0), 9 (1000.0)	Power line: 1-14, 2-12, 4-15, 6-13, 7-8, 11-23, 15-17, 17-22; PV: 1(0.35), 4(0.86), 15(1.68); WT: 2(2.50), 9(2.50), 14(1.51); PtH: 8 (6.00), 9 (4.63); HS: 1 (723.0), 3 (172.7), 4 (287.9), 5 (574.1), 6 (778.4), 8 (1305.2), 9 (1321.9)	Power line: 4-16, 5-24, 7-19, 10-16, 18-24, 20-24; substation: 24; PV: 1(0.35), 4(2.14), 15(1.68), 19(0.32); WT: 2(3.50), 9(3.50), 14(3.16), 18(1.15), 20(0.09); PtH: 8 (6.00), 9 (6.69); HS: 1 (1004.6), 2 (230.3), 3 (207.3), 4 (322.4), 5 (574.1), 6 (778.4), 7 (430.5), 8 (2000.0), 9 (2000.0)
Case 2	Power line: 4-9, 3-23, 7-23, 10-23; PV: 1(0.35), 4(0.87); WT: 2(1.50), 9(1.43); PtH: 8 (2.10), 9 (2.86); HS: 1 (526.2), 4 (230.3), 5 (477.3), 8 (705.0), 9 (1000.0)	Power line: 1-14, 2-3, 2-12, 4-15, 6-13, 7-8, 10-16, 11-23, 15-17, 17-22; PV: 1(0.35), 4(1.16), 15(1.01); WT: 2(2.50), 9(2.50), 14(0.63); PtH: 8 (4.60), 9 (6.00); HS: 1 (801.5), 3 (172.7), 4 (287.9), 5 (477.3), 6 (718.5), 8 (1366.0), 9 (1500.0)	Power line: 4-16, 5-24, 7-19, 15-19, 18-24, 20-24; substation: 24; PV: 1(0.35), 4(2.33), 15(1.01); WT: 2(3.50), 9(3.50), 14(1.90), 18(1.11), 20(0.03); PtH: 8 (6.08), 9 (6.28); HS: 1 (801.5), 2 (526.2), 3 (207.3), 4 (322.4), 5 (477.3), 6 (718.5), 7 (172.7), 8 (1366.0), 9 (2000.0)	

Note: planning decisions for PV (MW), WT (MW), PtH (MW), and HS (kg) are presented as $x(y)$, x and y refer to the node mark and installed capacity, respectively. Non-bold nodes and bold nodes represent the PDS and HES nodes, respectively.

C. 54-node System

The proposed model is further tested on a modified 54-node PDS with a 9-node HES, which contains 4 substations (35 kV), 50 power load nodes, 17 existing power lines, 46 candidate power lines, 2 HGSs, 7 HRSSs, and 13 roads. In HES, 2 HGS nodes 8 and 9 are connected to PDS nodes 9 and 16, respectively. To relieve the computation burden, six time periods are considered for PDS in each day ($N_{\tau}=6$, $\Delta_{\tau}=4$ hours). Long-term power and hydrogen load growth scenarios are utilized. More data related to the test system can

refer to [33]. The optimality gap in this system is set to be 5%, and the computation time is 22.24 hours. The cost comparisons of five cases for 54-node PDS and 9-node HES are shown in Table XIII. In the 54-node system, we can obtain a similar conclusion to those in the 8-node and 24-node PDSs. All the test systems verify that the proposed multi-stage stochastic IPDHS co-planning model can coordinate the PDS expansion and HES allocation to bring a cost saving and decrease the investment risks under long-term load growth uncertainties.

TABLE XIII
COST COMPARISON OF FIVE CASES FOR 54-NODE PDS AND 9-NODE HES

Type		Cost (\$10 ⁵)				
		Case 1	Case 2	Case 3	Case 4	Case 5
PDS	Investment	32.99	32.88	32.78	34.36	32.28
	Maintenance	19.88	19.42	19.69	19.98	19.90
	Production	350.00	351.46	350.15	352.76	349.88
	Curtailement	1.17	1.55	1.14	1.36	1.16
	Total	404.04	405.31	403.76	408.46	403.22
HES	Investment	20.42	21.16	20.16	17.15	20.42
	Maintenance	12.26	12.79	12.09	10.08	12.17
	Production	54.57	53.56	56.49	58.19	54.53
	Curtailement	0	0	0.08	0	0
	Total	87.25	87.51	88.82	85.42	87.12
IPDHS	Total	491.29	492.82	492.58	493.88	490.34

VI. CONCLUSION

This paper proposes a multi-stage stochastic IPDHS co-planning model under long-term load growth uncertainties. In the planning model, the PDS expansion and the HES including hydrogen production, transportation and storage sectors are comprehensively considered. Wherein, substations, power lines, PVs, WTs, PTHs, and HSs are invested to supply the uncertain power and hydrogen loads over the planning horizon. To achieve a more flexible decision-making process under load growth uncertainties, the multi-stage stochastic planning model is utilized.

Numerical results verify the coordination of PDS, and HES can reduce the total planning cost and achieve more efficient resource allocation. Additionally, the multi-stage stochastic model can provide a flexible planning decision tree and outperform the two-stage stochastic model. In future work, we will investigate more efficient modeling methods and solution techniques to improve the computational performance of the planning model. In addition, more technical features for the hydrogen system such as pipeline transmission and seasonal storage will also be considered. Another direction is to design a decentralized planning framework to preserve the data privacy of different planners.

REFERENCES

- [1] R. Palma-Behnke, J. Vega-Herrera, F. Valencia *et al.*, "Synthetic time series generation model for analysis of power system operation and expansion with high renewable energy penetration," *Journal of Modern Power Systems and Clean Energy*, vol. 9, no. 4, pp. 849-858, Jul. 2021.
- [2] S. Wang, Y. Dong, Q. Zhao *et al.*, "Bi-level multi-objective joint planning of distribution networks considering uncertainties," *Journal of Modern Power Systems and Clean Energy*, vol. 10, no. 6, pp. 1599-1613, Nov. 2022.
- [3] G. Pan, W. Gu, Q. Hu *et al.*, "Cost and low-carbon competitiveness of electrolytic hydrogen in China," *Energy & Environmental Science*, vol. 14, no. 9, pp. 4868-4881, Jul. 2021.
- [4] Z. Wang, T. Ding, W. Jia *et al.*, "Multi-period restoration model for integrated power-hydrogen systems considering transportation states," *IEEE Transactions on Industry Application*, vol. 58, no. 2, pp. 2694-2706, Mar. 2022.
- [5] P. Xiao, W. Hu, X. Xu *et al.*, "Optimal operation of a wind-electrolytic hydrogen storage system in the electricity/hydrogen markets," *International Journal of Hydrogen Energy*, vol. 45, no. 46, pp. 24412-24423, Sept. 2020.
- [6] M. Ban, W. Bai, W. Song *et al.*, "Optimal scheduling for integrated energy-mobility systems based on renewable-to-hydrogen stations and tank truck fleets," *IEEE Transactions on Industry Application*, vol. 58, no. 2, pp. 2666-2676, Mar. 2022.
- [7] C. Shao, C. Feng, M. Shahidehpour *et al.*, "Optimal stochastic operation of integrated electric power and renewable energy with vehicle-based hydrogen energy system," *IEEE Transactions on Power Systems*, vol. 36, no. 5, pp. 4310-4321, Sept. 2021.
- [8] W. Dong, C. Shao, C. Feng *et al.*, "Cooperative operation of power and hydrogen energy systems with HFCV demand response," *IEEE Transactions on Industry Application*, vol. 58, no. 2, pp. 2630-2639, Mar. 2022.
- [9] D. Zhao, M. Zhou, J. Wang *et al.*, "Dispatching fuel-cell hybrid electric vehicles toward transportation and energy systems integration," *CSEE Journal of Power and Energy Systems*. doi: 10.17775/CSEEJPES.2020.03640
- [10] M. Asensio, P. M. de Quevedo, G. Munoz-Delgado *et al.*, "Joint distribution network and renewable energy expansion planning considering demand response and energy storage—part I: stochastic programming model," *IEEE Transactions on Smart Grid*, vol. 9, no. 2, pp. 655-666, Feb. 2018.
- [11] Z. Wu, Q. Sun, W. Gu *et al.*, "AC/DC hybrid distribution system expansion planning under long-term uncertainty considering flexible investment," *IEEE Access*, vol. 8, pp. 94956-94967, Aug. 2020.
- [12] R. Li, W. Wang, X. Wu *et al.*, "Cooperative planning model of renewable energy sources and energy storage units in active distribution systems: A bi-level model and Pareto analysis," *Energy*, vol. 168, pp. 30-42, Feb. 2019.
- [13] Q. Sun, Z. Wu, W. Gu *et al.*, "Flexible expansion planning of distribution system integrating multiple renewable energy sources: an approximate dynamic programming approach," *Energy*, vol. 226, p. 120367, Jul. 2021.
- [14] P. Liu, Z. Wu, W. Gu *et al.*, "Security-constrained AC-DC hybrid distribution system expansion planning with high penetration of renewable energy," *International Journal of Electrical Power and Energy Systems*, vol. 142, p. 108285, May 2022.
- [15] J. M. Home-Ortiz, M. Pourakbari-Kasmaei, M. Lehtonen *et al.*, "A mixed integer conic model for distribution expansion planning: matheuristic approach," *IEEE Transactions on Smart Grid*, vol. 11, no. 5, pp. 3932-3943, Sept. 2020.
- [16] L. Zheng, J. Wang, Y. Yu *et al.*, "On the consistency of renewable-to-hydrogen pricing," *CSEE Journal of Power and Energy Systems*, vol. 8, no. 2, pp. 392-402, Mar. 2022.
- [17] G. Pan, W. Gu, Y. Lu *et al.*, "Optimal planning for electricity-hydrogen integrated energy system considering power to hydrogen and heat and seasonal storage," *IEEE Transactions on Sustainable Energy*, vol. 11, no. 4, pp. 2662-2676, Oct. 2020.
- [18] Y. Xiao, X. Wang, P. Pinson *et al.*, "A local energy market for electricity and hydrogen," *IEEE Transactions on Power Systems*, vol. 33, no. 4, pp. 3898-3908, Jul. 2018.

- [19] G. He, D. S. Mallapragada, A. Bose *et al.*, “Hydrogen supply chain planning with flexible transmission and storage scheduling,” *IEEE Transactions on Sustainable Energy*, vol. 12, no. 3, pp. 1730-1740, Jul. 2021.
- [20] W. Gan, M. Yan, W. Yao *et al.*, “Multi-network coordinated hydrogen supply infrastructure planning for the integration of hydrogen vehicles and renewable energy,” *IEEE Transactions on Industry Application*, vol. 58, no. 2, pp. 2875-2886, Mar. 2022.
- [21] S. Wang and R. Bo, “Joint planning of electricity transmission and hydrogen transportation networks,” *IEEE Transactions on Industry Application*, vol. 58, no. 2, pp. 2887-2897, Mar. 2022.
- [22] C. Yun and L. Dong, “Planning method for multi-regional interconnected energy stations of electricity and hydrogen,” in *Proceedings of 2021 China International Conference on Electricity Distribution (CICED)*, Shanghai, China, Apr. 2021, pp. 1-7.
- [23] Z. Wu, Q. Sun, Y. Lu *et al.*, “Distributed chance-constrained based total energy supply capability evaluation method for integrated power and natural gas system,” *International Journal of Electrical Power and Energy Systems*, vol. 141, p. 108193, Apr. 2022.
- [24] H. Yang, C. Li, M. Shahidehpour *et al.*, “Multistage expansion planning of integrated biogas and electric power delivery system considering the regional availability of biomass,” *IEEE Transactions on Sustainable Energy*, vol. 12, no. 2, pp. 920-930, Apr. 2021.
- [25] M. Farivar and S. H. Low, “Branch flow model: relaxations and convexification—part I,” *IEEE Transactions on Power Systems*, vol. 28, no. 3, pp. 2554-2564, Aug. 2013.
- [26] A. Ben-Tal and A. Nemirovski, “On polyhedral approximations of the second-order cone,” *Mathematics of Operations Research*, vol. 26, no. 2, pp. 193-205, May 2001.
- [27] R. A. Jabr, R. Singh, and B. C. Pal, “Minimum loss network reconfiguration using mixed-integer convex programming,” *IEEE Transactions on Power Systems*, vol. 27, no. 2, pp. 1106-1115, May 2012.
- [28] H. Qiu, W. Gu, P. Liu *et al.*, “Application of two-stage robust optimization theory in power system scheduling under uncertainties: a review and perspective,” *Energy*, vol. 251, p. 123942, Jul. 2022.
- [29] T. Ding, M. Qu, C. Huang *et al.*, “Multi-period active distribution network planning using multi-stage stochastic programming and nested decomposition by SDDIP,” *IEEE Transactions on Power Systems*, vol. 36, no. 3, pp. 2281-2292, May 2021.
- [30] T. Ding, Y. Hu and Z. Bie, “Multi-stage stochastic programming with nonanticipativity constraints for expansion of combined power and natural gas systems,” *IEEE Transactions on Power Systems*, vol. 33, no. 1, pp. 317-328, Jan. 2018.
- [31] S. Sannigrahi, S. R. Ghatak, and P. Acharjee, “Multi-scenario based bi-level coordinated planning of active distribution system under uncertain environment,” *IEEE Transactions on Industry Application*, vol. 56, no. 1, pp. 850-863, Jan. 2020.
- [32] P. M. de Quevedo, G. Muñoz-Delgado, and J. Contreras, “Impact of electric vehicles on the expansion planning of distribution systems considering renewable energy, storage, and charging stations,” *IEEE Transactions on Smart Grid*, vol. 10, no. 1, pp. 794-804, Jan. 2017.
- [33] Q. Sun. Test data of IPDHS [Online]. Available: <https://docs.google.com/spreadsheets/d/1Ugg820BLfAfhA2unCuRP0VEVxIeRY9-w/edit?usp=sharing&oid=113763688474220342932&rtpof=true&sd=true>
- Qirun Sun** received the B.E. degree in electrical engineering from Southeast University, Nanjing, China, in 2018. He is currently working toward the Ph.D. degree at the School of Electrical Engineering, Southeast University. His research interests include distribution system planning and integrated energy system resilience.
- Zhi Wu** received the B.Eng. degree in mathematics and the M.Sc. degree in electrical engineering from Southeast University, Nanjing, China, in 2009 and 2012, respectively, and the Ph.D. degree from the University of Birmingham, Birmingham, U.K., in 2016. He is currently an Associate Professor with the School of Electrical Engineering, Southeast University. His research interests include renewable energy, planning, and optimization techniques.
- Wei Gu** received the B.S. and Ph.D. degrees in electrical engineering from Southeast University, Nanjing, China, in 2001 and 2006, respectively. From 2009 to 2010, he was a Visiting Scholar with the Department of Electrical Engineering, Arizona State University, Tempe, USA. He is currently a Professor with the School of Electrical Engineering, Southeast University. He is the Director of the Institute of Distributed Generations and Active Distribution Networks. His research interests include distributed generations and micro-grids, and integrated energy system.
- Pengxiang Liu** received the B.S. degree in electrical engineering from Zhengzhou University, Zhengzhou, China, in 2017, and the M.Eng. degree in 2019 in electrical engineering from Southeast University, Nanjing, China, where he is currently working toward the Ph.D. degree with the School of Electrical Engineering. His research interests include multi-energy system optimization, operations research, and machine learning.
- Jingxuan Wang** received the B.Eng. degree in electrical engineering from Hohai University, Nanjing, China, in 2020. She is currently pursuing the master degree at the School of Electrical Engineering, Southeast University, Nanjing, China. Her research interests include integrated energy system optimization and operation research.
- Yuping Lu** received the Ph.D. degree in electrical engineering from the City University, U.K., in 2003. He is currently a Professor with the School of Electrical Engineering, Southeast University, Nanjing, China. His research interests include power system protection (especially digital relaying of generator transformer unit) and protection-and-control techniques of distribution systems.
- Shu Zheng** is currently pursuing the Ph.D. degree in electrical engineering from Southeast University, Nanjing, China. She is the Jiangsu Industry Professor in NARI Technology Development Co. Ltd. Her research interests include distribution network automation, AC/DC hybrid distribution network.
- Jingtao Zhao** is the Deputy General Manager of power distribution/agricultural power branch in NSRI Technology Development Co.Ltd. His research interests include distribution network automation, AC/DC hybrid distribution network, distributed generation/microgrid.